Delft University of Technology

Development of a hazard risk map for assessing pedestrian risk in urban flash floods
A case study in Cúcuta, Colombia

Corzo Perez, Gerald Augusto; Sanchez Tapiero, Diego Ivan; Contreras Martínez, Manuel Antonio; Zevenbergen, Chris

DOI
[10.1002/rvr2.78](https://doi.org/10.1002/rvr2.78)

Publication date
2024

Document Version
Final published version

Published in
River

Citation (APA)
Corzo Perez, G. A., Sanchez Tapiero, D. I., Contreras Martínez, M. A., & Zevenbergen, C. (2024). Development of a hazard risk map for assessing pedestrian risk in urban flash floods: A case study in Cúcuta, Colombia. *River*, *3*, 8-23. https://doi.org/10.1002/rvr2.78

Important note
To cite this publication, please use the final published version (if applicable).
Please check the document version above.

Copyright
Other than for strictly personal use, it is not permitted to download, forward or distribute the text or part of it, without the consent of the author(s) and/or copyright holder(s), unless the work is under an open content license such as Creative Commons.

Takedown policy
Please contact us and provide details if you believe this document breaches copyrights.
We will remove access to the work immediately and investigate your claim.

This work is downloaded from Delft University of Technology.
For technical reasons the number of authors shown on this cover page is limited to a maximum of 10.

RESEARCH ARTICLE

Development of a hazard risk map for assessing pedestrian risk in urban flash floods: A case study in Cúcuta, Colombia

Gerald Augusto Corzo Perez[1] | Diego Ivan Sanchez Tapiero[2] |
Manuel Antonio Contreras Martínez[2] | Chris Zevenbergen[3]

[1]IHE Delft Institute for Water Education, Hydroinformatics and Digital Innovation, Delft, The Netherlands

[2]Master in Environmental Engineering, Civil Engineering Program, Faculty of Engineering and Architecture, University of Pamplona, Pamplona, Colombia

[3]Faculty of Civil Engineering and Geosciences, Delft University of Technology, Delft, The Netherlands

Correspondence

Gerald Augusto Corzo Perez, IHE Delft Institute for Water Education, Hydroinformatics and Digital Innovation, Delft, The Netherlands.
Email: gerald.corzo@gmail.com and g.corzo@un-ihe.org

Diego Ivan Sanchez Tapiero, Master in Environmental Engineering, Civil Engineering Program, Faculty of Engineering and Architecture, University of Pamplona, Pamplona, Colombia.
Email: diego.sanchez@unipamplona.edu.co

Abstract

The rapid growth of impervious areas in urban basins worldwide has increased the number of impermeable surfaces in cities, leading to severe flooding and significant economic losses for civilians. This trend highlights the urgent need for methodologies that assess flood hazards and specifically address the direct impact on pedestrians, which is often overlooked in traditional flood hazard analyses. This study aims to evaluate a methodology for assessing the risk to pedestrians from hydrodynamic forces during urban floods, with a specific focus on Cúcuta, Colombia. The methodology couples research outcomes from other studies on the impact of floodwaters on individuals of different ages and sizes with 1D/2D hydrological modeling. Advanced computational algorithms for image recognition were used to measure water levels at 5-s intervals on November 6, 2020, using drones for digital elevation model data collection. In Cúcuta, where flood risk is high and drainage infrastructure is limited, the PCSWMM (Computer-based Urban Stormwater Management Model) was calibrated and validated to simulate extreme flood events. The model incorporated urban infrastructure details and geomorphological parameters of Cúcuta's urban basin. Four return periods (5, 10, 50, 100), with extreme rainfall of 3 h, were used to estimate the variability of the risk map. The output of the model was analyzed, and an integrated and time-varying comparison of the results was done. Results show that the regions of high-water depth and high velocity could vary significantly along the duration of the different extreme events. Also, from 5 to 100 years return period, the percentage of area at risk increased from 9.6% to 16.6%. The pedestrian sensitivity appears much higher than the increase in velocities or water depth individually. This study identified medium to high-risk locations, which are dynamic in time. We can conclude dynamics are spatiotemporal, and the added information layer of pedestrians brings vulnerability information that is also dynamic. Areas of immediate concern in Cúcuta can enhance pedestrian safety during flash flood events. The spatiotemporal variation of patterns requires further studies to map trajectories and sequences that machine learning models could capture.

KEYWORDS

hazard and risk mapping, pedestrian risk, urban flood

1 | INTRODUCTION

Global urban flooding events and associated risks are an escalating concern, particularly in developing countries where the dangers are less understood and studied (Nkwunonwo et al., 2020). The United Nations' "World Water Development Report 2020: Water and Climate Change" highlights a significant increase in flooding and precipitation due to climate change, with a rate four times higher than in 1980 (United Nations [UN], 2020). This phenomenon has particularly affected regions like China and Southeast Asia, impacting over 100 million people annually since 2006 (Liu et al., 2019). Moreover, the World Meteorological Organization (WMO) reports that 79% of natural disasters from 1970 to 2012 involved flooding, leading to the majority of deaths and economic losses during this period (OMM, 2014).

The specific risk to pedestrians in flood scenarios is a critical yet often overlooked aspect of urban flood studies. Research has shown that walking and driving in floodwaters are primary dangers during floods (Tascón-González et al., 2020), with the combination of flow velocity and depth posing significant threats (Altomare et al., 2020). Although flood hazard maps are commonly used to estimate dangers, they frequently fail to address the unique vulnerabilities of pedestrians and drivers (Arosio et al., 2021; Kvočka et al., 2016). The complexity of assessing pedestrian safety extends to evaluating individual risks in varying environmental conditions (Xu et al., 2017) and understanding the nuances of pedestrian behavior during floods (Shirvani & Kesserwani, 2021).

The rapid urbanization in Latin America has led to significant socioeconomic, demographic, and environmental challenges, with urban floods being the most frequent and devastating disaster. The Center for Research on the Epidemiology of Disasters (CRED) projects that 68% of the world's population will reside in urban areas by 2050, exacerbating these challenges. Between 1990 and 2017, floods in Latin America caused over 5689.5 deaths and economic losses exceeding 105 billion USD, affecting more than 87 million people (Aragón-Durand, 2014).

These statistics highlight not only the direct impact of floods but also their indirect effects, such as educational delays and increased disease rates.

In Cúcuta, Colombia, urban floods from pluvial sources have repeatedly caused severe disruptions, continuously reported by news media (Figure 1). Traditional mitigation approaches, including expanding drainage networks and constructing ad hoc rainwater channels, have proven expensive and have inadvertently increased flood risks by altering natural water processes.

As climate change continues to increase the frequency and intensity of convective rains and floods worldwide (Pregnolato et al., 2017), there is an urgent need for hydrological analyses that incorporate these changes. Early attempts to integrate climate change projections using Global Climate Models have been simplistic, often neglecting specific risks to pedestrians (Maimone et al., 2019). Our study addresses this gap by introducing a novel methodology focused on pedestrian risk in urban flooding scenarios, specifically applied to the context of Cúcuta, Colombia.

Recent advancements in flood risk assessment have predominantly focused on mechanics-based analysis and regional-scale evaluation (Kvočka et al., 2016). However, these methodologies often overlook the critical aspect of pedestrian safety, particularly at marked crossings and within urban environments. This gap is notable in the lack of comprehensive assessment at the household level, which is crucial for evaluating vulnerability and risk in pedestrian-centric areas.

The impact of climate change on flood protection systems has garnered considerable attention, yet the methodologies used frequently omit explicit considerations for pedestrian safety infrastructure. This omission indicates a significant gap, as novel approaches to environmental assessment of pedestrian injury suggest the need for a more robust inventory of pedestrian safety infrastructure (Xu et al., 2017). Additionally, the concept of "safety in numbers" at intersections, where higher pedestrian traffic is presumed to lead to greater safety, raises concerns about the current methodologies' ability to assess flood risks in pedestrian-heavy areas adequately (Xu et al., 2017).

FIGURE 1 Pluvial Floods in the city of Cúcuta (Colombia). *Source*: La Opinion, 2020.

Further complicating this issue is the observed pedestrian gap acceptance behavior in street designs that incorporate elements of shared space, underscoring the need for methodologies that integrate pedestrian behavior into flood risk assessments. This integration is particularly critical in climate change, which alters the dynamics of flood protection systems and, consequently, the safety of pedestrian infrastructure.

In conclusion, while there have been significant advancements in flood risk assessment, current methodologies exhibit a notable deficiency in comprehensively integrating pedestrian safety considerations. This oversight is particularly evident in the context of climate change impacts and at the regional and household levels. Future methodologies must endeavor to fill these gaps, ensuring a holistic approach that adequately addresses the safety of pedestrians, especially in areas prone to flooding.

2 | METHODOLOGY

The methodology employed in this research was structured into five phases (Figure 2), progressing from model construction to the development of pedestrian hazard maps. Each phase is outlined below.

2.1 | Phase 1: Data collection of precipitation

Meteorological data for the study area were collected from the rainfall regimes recorded by the Institute of Hydrology, Meteorology, and Environmental Studies (IDEAM)

meteorological stations. The pluviometric data from the Camilo Daza Airport station were selected due to its extensive historical records and proximity to the study area, adhering to the guidelines established by the WMO. Maximum 24-h monthly precipitation data from 1970 to 2021 were analyzed using the Gumbel probability distribution and the Intensity–Duration–Frequency (IDF) curves were generated based on Bernard's method (Bernard, 1932).

2.2 | Phase 2: Obtaining the digital elevation model (DEM)

The DEM was acquired using a Phantom 3 Advance drone, aligning with the increasing application of UAVs in topographic data collection (Abbas & Jaber, 2020; Escalante et al., 2016). The process followed the methodology proposed by Nájera-Ramos (2021), involving flight planning, image capture, control point georeferencing, and generation of the DEM using Agisoft Metashape software.

2.3 | Phase 3: Model setup

The stormwater management modeling in this study was performed using PCSWMM software (version 7.4.3240) (Hamouz et al., 2020). The model was based on the solution of the 1D Saint-Venant equations (Mohd Sidek et al., 2021) and incorporated GIS data. To create the input layers, the parameters for the 1D model, including connections, conduits, drains, and subbasins, were exported to PCSWMM
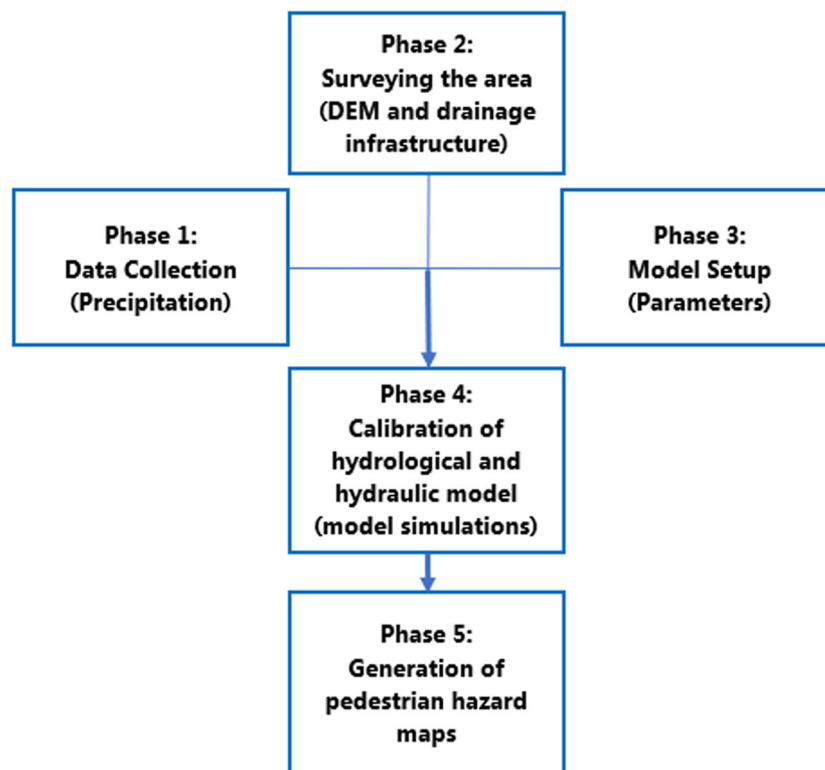

FIGURE 2 Phases of the methodology.

from a GIS. The Curve Number (CN) method was used to estimate runoff (Diaz Carvajal & Mercado Fernández, 2017).

The hydrological and hydraulic models used a two-dimensional configuration with different types and sizes of meshes. The meshes were carefully analyzed to find an acceptable time step for the model and prevent numerical instabilities. The two-dimensional model was configured using three 2D meshes representing the Bogotá channel, the permeable areas, and the roads of the study area.

The Bogotá channel was created with a directional mesh at a resolution of 3 m and a Manning roughness coefficient of 0.02 weighted for concrete and rock. In the permeable areas, a hexagonal mesh with a 5 m resolution and a weighted Manning coefficient of 0.285 was used. Different coverages were presented in the permeable areas. For the roads, a coefficient of 0.011 for asphalt pavement and 0.012 for concrete was implemented at a smaller resolution of 2 m.

The topographic representation of the terrain in the hydrological and hydraulic model was carried out through a layer of 2D connections using elevation data from the DEM. This created a 2D mesh of connections and cells based on the attributes of the meshes mentioned above. The type and size of the meshes were obtained by conducting different tests in the model until a continuity error and routing of less than 1% were achieved. This was possible by modifying the time step (Δt) for flow routing and calculating it using the Courant condition. The smallest conduit in the model determined the Δt, and a smaller value was inserted to prevent numerical instabilities and high continuity errors in the modeling (James et al., 2010). This is an acceptable value for numerical solutions in PCSWMM (Computational Hydraulics Int [CHI], 2023).

Water depth data was used to calibrate the model by *analysing* image frames from videos capturing flood occurrences during selected rain events in specific areas of the basin. Advanced computer vision techniques in Matlab were used to extract and interpret imagery from various electronic sources, combining human measurements in the field with video and photo recording for a complete mapping of measurements and flood areas. This process generated detailed observed hydrograph data for the study area at 5-s intervals during the November 6, 2020, rainfall event. The data incorporates both the duration of the precipitation event and the measured flow heights, providing a robust basis for the model's calibration (Isidoro et al., 2021). Water depth data was obtained from video footage and analyzed using computer vision techniques in Matlab (Isidoro et al., 2021; Kim et al., 2011).

The Sensitivity-based Radio Tuning Calibration (SRTC) tool in PCSWMM was used for calibrating (Parameter adjustment; Castro et al., 2022) see details in the following section.

2.4 | Phase 4: Calibration of the hydrological and hydraulic model

The methodology for representing rainfall within the computational model involved a meticulous setup and calibration process to ensure accuracy and reliability in flood prediction. This was achieved by integrating IDF curves into the PCSWMM software. Utilizing the storm tool feature, design hyetographs were meticulously crafted employing the Chicago storm distribution method. These hyetographs were tailored for specific return periods of 5, 10, 50, and 100 years, each with a designated maximum rainfall duration of 180 min (3 h). This duration was intentionally set to exceed the basin's concentration time of 58 min. The rationale behind this decision was to model flood scenarios driven by rainfall intensity rather than by flow accumulation in urban pathways, ensuring a realistic simulation of urban flooding dynamics.

The choice of a 3-h rainfall duration, beyond the basin's concentration time, was strategic to capture the full impact of intense rainfall events, thereby providing a comprehensive understanding of flood risks under various scenarios. The concentration time itself was derived from the geomorphological parameters of the study area. This parameter is critical as it represents the time required for a water droplet to travel from the most distant point of the basin to the discharge point, offering insights into the hydrological response of the basin.

To further refine the model's accuracy, a calibration process was undertaken. This process involved adjusting the model parameters to align with observed data, ensuring that the model's predictions of flood extent, depth, and duration closely match real-world observations. The calibration was supported by historical rainfall and flood records, providing a robust framework for validating the model's performance. This meticulous methodology aimed to establish a reliable computational model capable of simulating urban flood scenarios with high precision, thereby contributing valuable insights for urban planning and flood risk management (Avila & Avila, 2016).

2.5 | Phase 5: Generation of pedestrian hazard maps in GIS

Pedestrian hazard zones were determined using criteria from Martínez Gomariz (2016) and validated against numerical models (Russo, 2009). The 1D–2D hydrological and hydraulic model data were imported into QGIS, and the criteria for pedestrian hazard were applied to each cell to represent hazard levels.

Table 1 categorizes the levels of pedestrian hazard in flood conditions based on water depth and velocity. Three hazard levels are defined: low, medium, and high.

TABLE 1 Pedestrian hazard levels.

Hazard level	Adopted criteria	Color
Low	$y \leq 0.5$ m y $(v \times y) \leq 0.16$ m^2/s	
Medium	$y \leq 0.5$ m y 0.16 m^2/s $< (v \times y) \leq 0.22$ m^2/s	
High	$y > 0.5$ m ó $(v \times y) > 0.22$ m^2/s ó $v > 1.88$ m/s	

The "low" level is characterized by water depths of 0.5 m or less and a product of depth and velocity not exceeding 0.16 m²/s. The "medium" level is assigned when water depth remains at or below 0.5 m, but the product of depth and velocity falls between 0.16 and 0.22 m²/s. A "high" hazard level is determined when water depth exceeds 0.5 m, the product of depth and velocity is greater than 0.22 m²/s, or the velocity alone surpasses 1.88 m/s. This classification aids in assessing and visualizing flood risks to pedestrians, facilitating informed urban flood management and safety planning.

3 | CASE STUDY: CÚCUTA, COLOMBIA

The study area under consideration is in the northeastern part (7°55′17.19″N, 72°30′3.22″W) of Cúcuta, Colombia. The area is bounded by Avenida 4 between Calle 16N and Calle 23N in the northwest and by Calle 9ª N between Avenida Guiamaral and Libertadores in the southeast. The densely populated region features mixed land use, including substantial commercial and industrial activities. Despite being close to a major rainwater drainage canal that handles significant runoff from the city, the local rainwater drainage system is notably deficient.

In recent years, this zone has experienced urban flooding characterized by high water velocities and levels, posing significant risks to pedestrians. Three primary factors contribute to these flooding events. First, the coverage of the stormwater drainage system in this area is insufficient. Second, the lack of regular cleaning and maintenance has led to the clogging of many runoff grates. Lastly, morphological phenomena of the streets and sidewalks cause the accumulation of rainwater from other areas. These factors create severe flooding during extreme rainfall events, leading to high water levels that disrupt vehicular and pedestrian circulation. Such conditions not only pose a threat to the physical safety of residents but also cause damage to surrounding infrastructure.

This case study area is emblematic of the challenges faced in urban flood management, particularly in pedestrian safety. The application of the developed methodology in this study area aims to provide a comprehensive analysis of flood risks, with a focus on identifying and mitigating hazards to pedestrians. The findings from Cúcuta will offer valuable insights for urban planners and decision-makers, contributing to developing more resilient and safer urban environments.

3.1 | Drainage system in the study area

As previously mentioned, the drainage system in the study area has not been well planned. Few pipes and channels carry the runoff, leading to sudden flooding in various sectors. Currently, the system consists of concrete pipes with diameters of 0.61 and 0.84 m, collecting rainwater from the northwest of the study area to the Bogotá canal as the discharge point. On Avenida 2 Norte, a closed rectangular concrete channel is 1.85 m wide by 1 m high, discharging into the 0.84 m diameter pipe. In the Gratamira neighborhood, the Zulima neighborhood, and the flow along Avenida Libertadores, the runoff is captured by pipes with diameters of 0.91 and 1.27 m in concrete, installed on the left side of Avenida Libertadores up to Calle 18 Norte, where it crosses to the right side of this avenue until it discharges into the Bogotá canal, as shown in Figure 3b.

4 | RESULTS

4.1 | Phase 1: Data collection of precipitation

The study area, characterized by bimodal rainfall periods, experiences extreme precipitation events, influenced by El Niño and La Niña climatic phenomena. Annual maximum precipitation depths exceeded 168 mm, with the highest daily depths ranging from 118.1 to 168.4 mm, predominantly occurring in April, October, and November. Utilizing Gumbel's probability distribution, the maximum probable precipitation was determined to be 75.3 mm. This was derived from the probabilistic variables calculated ($S = 24.638$, $\alpha = 19.210$ mm, and $\mu = 64.251$ mm).

Daily maximum precipitations were computed using the 24-h rainfall coefficients proposed by D. F. Campos in 1978, along with fixed interval values for each return period, to ascertain rain intensities over various durations. These intensities were used to develop IDF curves using Bernard's established formula. The mathematical expression generated for the Cúcuta IDF curves with the analyzed data from the Camilo Daza Airport station is as follows:

$$I = [298.217 * Tr \wedge (0.168)]/D \wedge (0.616) \text{ mm/hr.} \quad (1)$$

Equation (1) Incorporates the values for return periods and durations in minutes, producing the IDF curves as depicted in Figure 4.

IDF curves provided by IDEAM for the Camilo Daza Airport station were downloaded (Figure 5). These curves were updated in December 2016 by the GIREH group of the National University, using pluviometric data from 1973 to 2010. The curves were estimated using the Gumbel distribution with the L-Moments method and employed four methodologies for the estimation of generalized curves, determining the factors C1, X0, and C2 for each return period to calculate the intensity of rainfall for a given duration.

The initial results from the hydraulic and hydrological model provide critical insights into the dynamics of the existing drainage systems in the study area of Cúcuta, particularly under conditions of heavy precipitation when these systems exceed their hydraulic capacity. The model
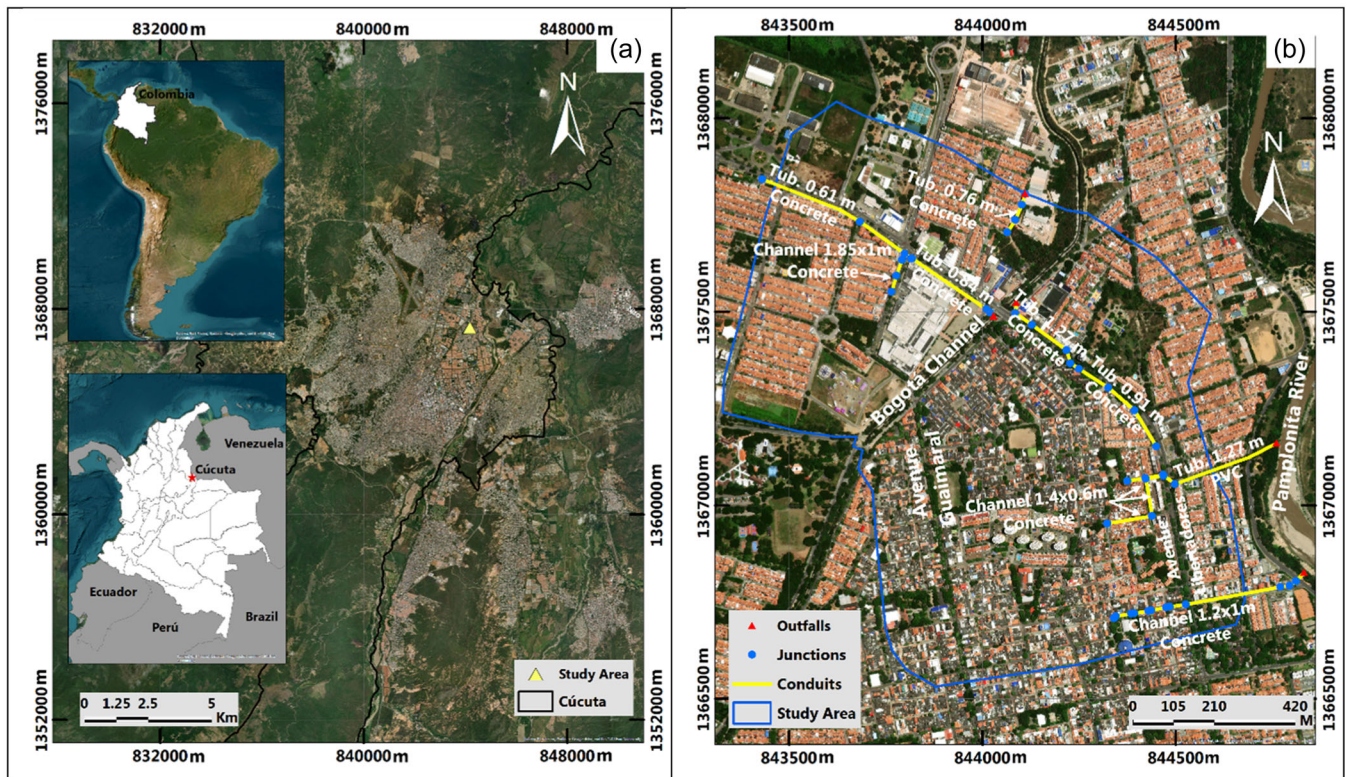
FIGURE 3 (a) Study Area, Cúcuta (Colombia), (b) drainage system. *Source*: Authors.
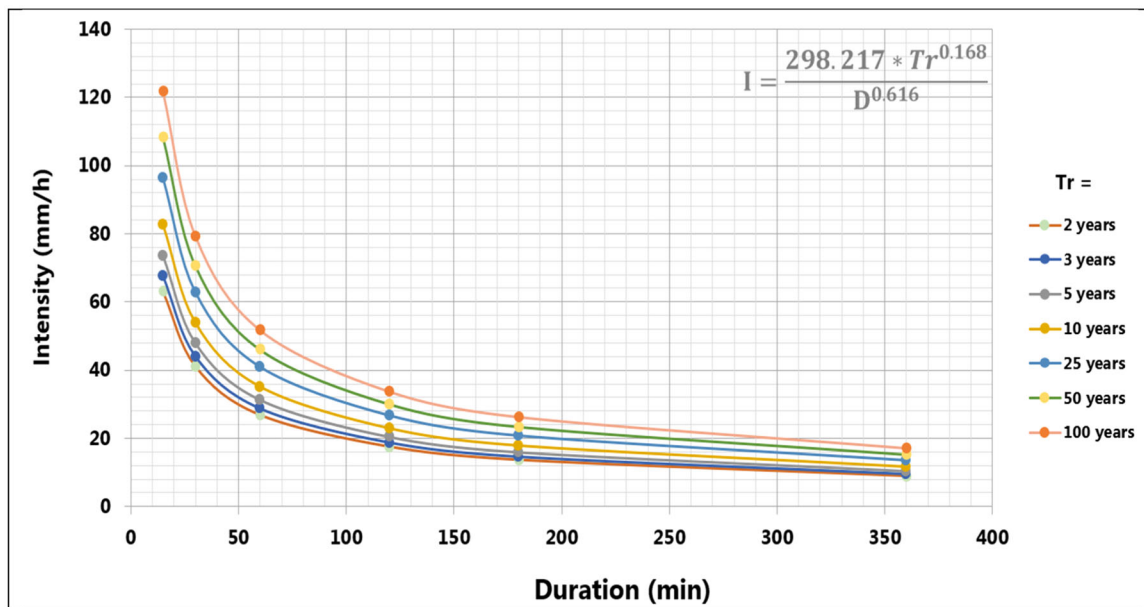

$$I = \frac{298.217 * Tr^{0.168}}{D^{0.616}}$$

FIGURE 4 Generated intensity–duration–frequency curves. *Source*: Authors.

effectively captured instances where the drainage system became overwhelmed, leading to rainwater emerging from wells and grates and contributing to surface runoff.

A comparison of the IDF curves generated using Bernard's mathematical expression and those provided by

IDEAM for the Camilo Daza Airport station is shown in Figure 6. The blue curves represent those generated by the authors, while the orange curves are those supplied by IDEAM. It is evident that the IDEAM curves indicate higher rainfall intensities for the various return periods
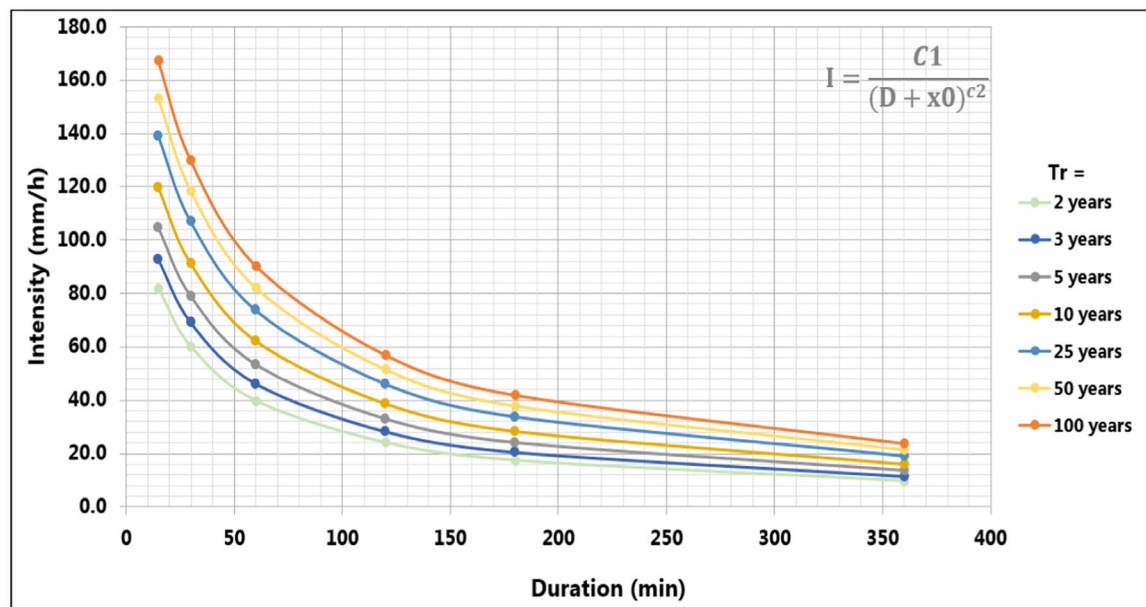
The equation shown in the figure:
$$I = \frac{C1}{(D + x0)^{c2}}$$

FIGURE 5 Downloaded intensity–duration–frequency curves. *Source*: IDEAM.
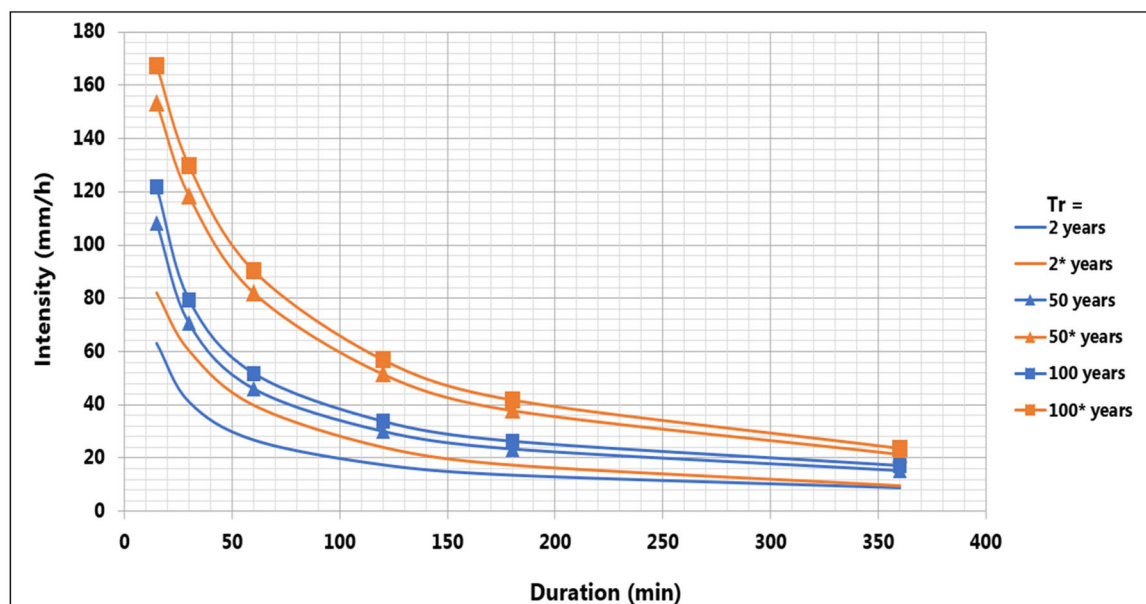

FIGURE 6 Generated Intensity–Duration–Frequency curves versus IDEAM curves. *Source*: Authors.

(2, 50, and 100 years). Additionally, the percentage error was calculated between the values determined by the mathematical expression and those calculated by IDEAM's equation for the station, revealing that for 2- and 3-year return periods, the error ranges between 20% and 30%, and for other periods (5, 10, 25, 50, and 100 years), the error remains consistent at 40%. Consequently, the IDEAM curves were chosen for flood modeling and generating hazard maps for the study area, as they account for more intense rainfall, aligning with the recent trends of significant precipitation and resulting high-depth flooding observed in the area.

Key outcomes include detailed identification of the primary areas within the study zone that are prone to

flooding. The model quantified flood depths and flow velocities for different rainfall scenarios, which are crucial metrics in assessing pedestrian danger. These areas of high-water depth and velocity were pinpointed as significant flood spots, highlighting the potential risk zones for pedestrians.

4.2 | Phase 2: DEM

The DEM was generated through the processing of 1178 images captured over five drone flights. Five control points were established throughout the study area, which were georeferenced using GPS/RTK GNSS to enhance the

precision of the DEM in the post-processing software (Figure 7).

The image processing yielded a dense point cloud with over 81 million points, providing a detailed representation of the surface topography. Points corresponding to natural terrain were classified and segregated from those representing trees, structures, and other objects, ensuring that only relevant points were utilized for the DEM construction. Furthermore, the DEM was refined along the Bogotá channel, where drone imagery failed to capture accurate data due to tree coverage. Multiple points along the channel were collected with GPS/RTK, and a comprehensive surface was created in GIS for the entire channel. The resultant DEM was then sectioned to correspond to the channel's extent within the study area, integrating it with the created surface using GIS tools.

The finalized, corrected DEM had a pixel size of 17 cm and covered an area of 130.52 hectares. It exhibited an elevation of 275 m above sea level (masl) in the lower zones and a maximum elevation of 285 masl in the higher regions, as illustrated in Figure 8. The lowest areas of the generated DEM correspond to the Bogotá channel base and Tasajero
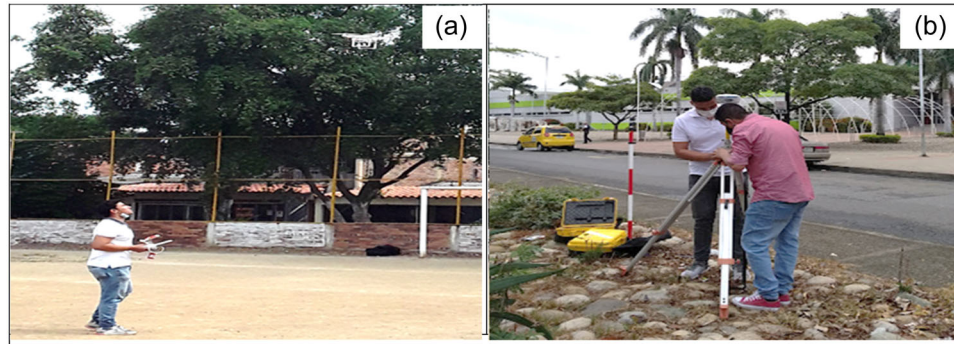

FIGURE 7 Fieldwork for the generation of the digital elevation model: (a) drone flight for image capture, (b) georeferencing of control points. *Source*: Authors.
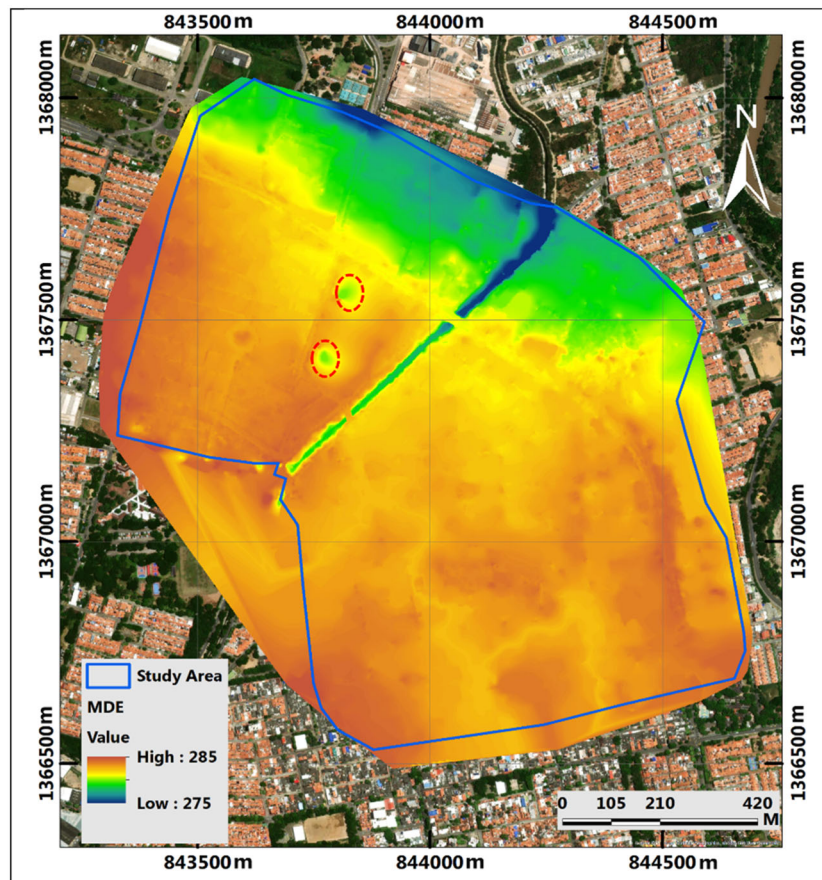

FIGURE 8 Improved digital elevation model of the study area. *Source*: Authors.

and Niza neighborhoods. Additionally, the model revealed two low points on Avenida 2 Norte near Unicentro, which are entrances to the subterranean parking of the shopping center. The neighborhood of Prados del Norte was identified as the highest elevation zone within the study area.

4.3 | Phase 3: Model setup

The constructed 1D–2D hydrological and hydraulic model in PCSWMM facilitated the representation of existing drainage networks and their interaction with the streets during flooding events. The 1D hydraulic model comprised 44 connections, representing inspection wells and inlets, and 39 conduits, both open and closed, leading to final emissaries which identify discharge points into the Bogotá channel and the Pamplonita River. The hydrological model consisted of 474 subbasins contributing runoff to the system.

The comprehensive view of the 1D–2D model (Figure 9a) displays the complete setup, with surface runoff flowing within the area to the discharge points (shown in brown), preventing flood accumulation. The 2D emissaries are located in the eastern and northeastern zones of the model, where most of the catchment's runoff drains toward the

Tasajero and Niza neighborhoods. Figure 9b illustrates the meshes created for the flow modeling in permeable areas, the channel, and streets, with a hexagonal mesh for permeable sectors, a directional mesh for the Bogotá channel, and a finer hexagonal mesh for urban streets to enhance precision in surface runoff modeling. The interaction between different 2D model meshes is finely tuned, accommodating sudden topological changes without computational errors. Figure 9c shows the established interaction between the 1D and 2D models, made possible by PCSWMM's direct connection approach, allowing for the seamless modeling of how 1D conduits discharge flow into a 2D connection and subsequently onto the free surface.

The design rainfall was configured using IDF curves provided by IDEAM for the Camilo Daza Airport meteorological station. Storm hyetographs were computed using the Chicago distribution method (Figure 10), taking into account parameters for each IDF and storm durations for selected return periods.

The hyetographs (Figure 10) indicate that for 5 and 10-year return periods, peak intensities exceed 130 and 150 mm/h, respectively. For larger return periods (50 and 100 years), the storm peak surpasses 180 and 210 mm/h, indicating the potential for severe urban flooding.
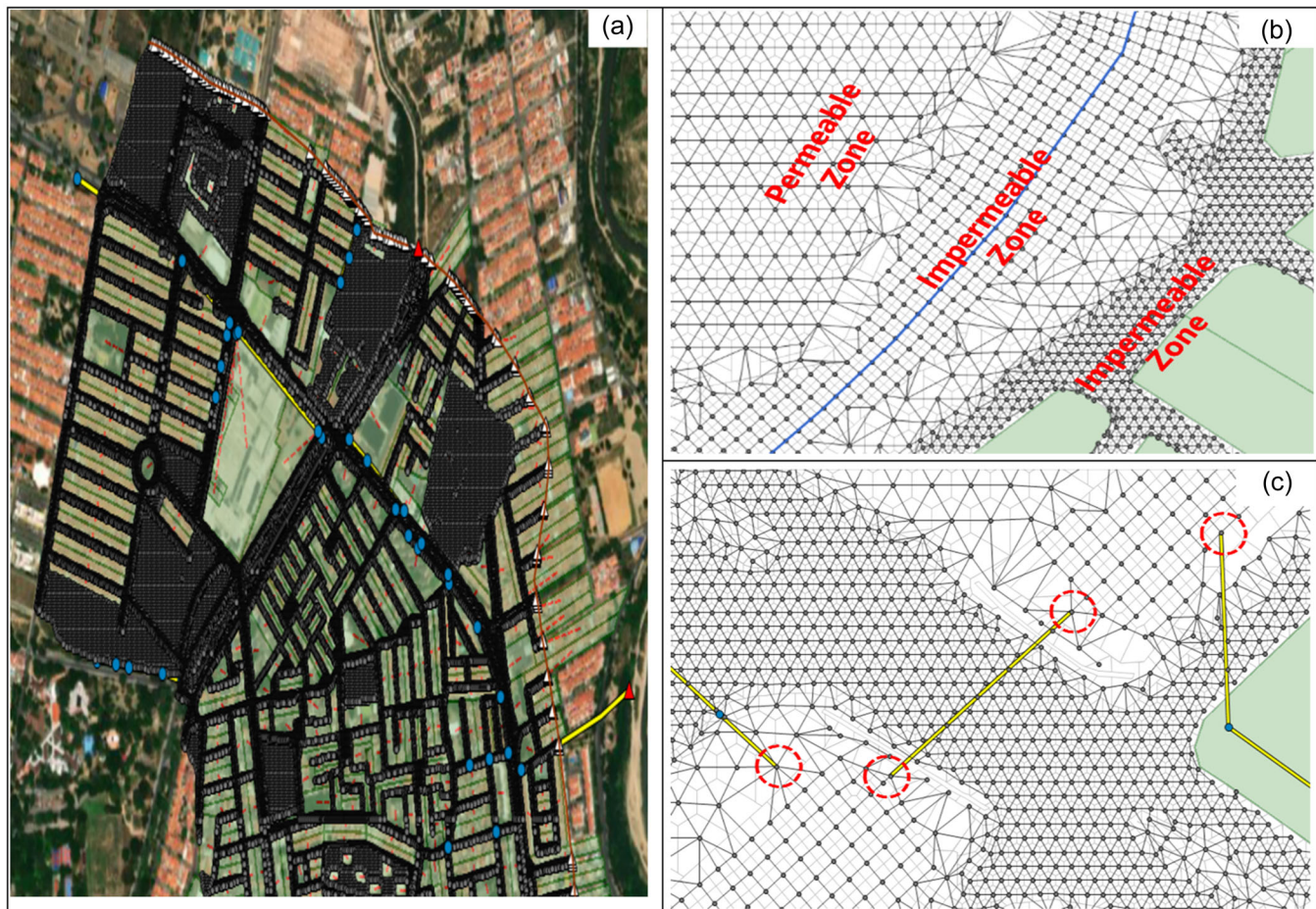

FIGURE 9 Hydrological and hydraulic 1D–2D model of the study area. (a) General view of the model, (b) types of meshes created, (c) direct 1D–2D connection. *Source*: Authors.
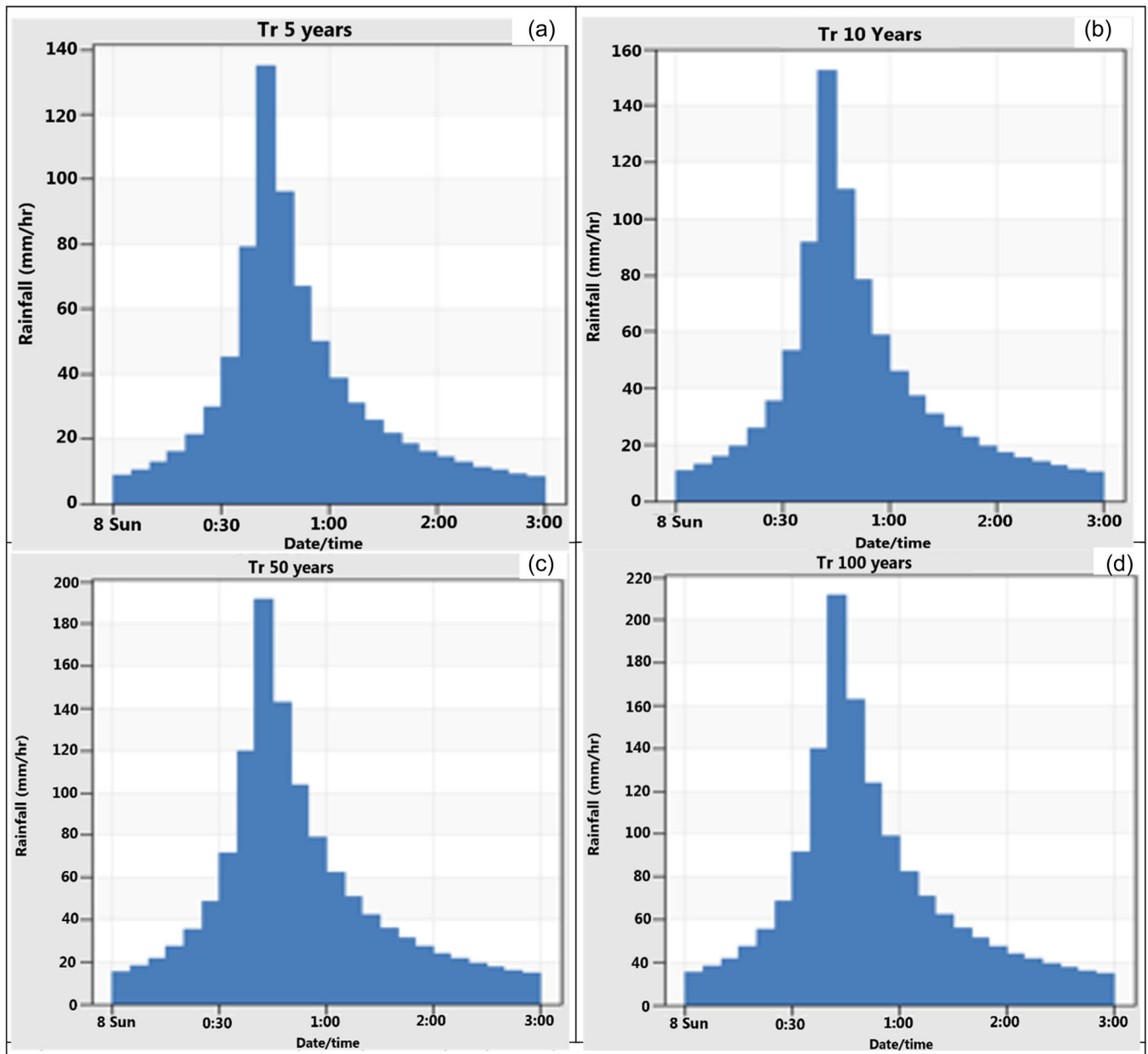
FIGURE 10 Storm hyetographs implemented in the study zone, (a) Tr 5 years, (b) Tr 10 years, (c) 50 years, and (d) 100 years. *Source*: Authors.

4.4 | Phase 4: Calibration of the hydrological and hydraulic model

The chosen site for model calibration was along Avenida Libertadores in Ciudad Jardín, where video surveillance captured significant flow accumulation during the November 6, 2020, event. Artificial vision analysis divided the over-3-h event into segments for precise correlation between observed water heights and precipitation timing. The artificial vision technique determined flow heights by pixel analysis, differentiating between the curb, road, and surface runoff (Figure 11).

The observed hydrogram was integrated into PCSWMM for calibration using the SRTC tool, adjusting parameters such as width, impermeability coefficient, Manning's coefficient for permeable zones, and the CN. The calibration yielded excellent results according to the Nash-Sutcliffe Efficiency and determination coefficient (R^2).

The final calibration (Figure 12) showed that adjusting the width and CN of subbasins improved the model's output. Although the peak of the hydrogram from calibration did not perfectly match observed data, with a maximum discrepancy of approximately 5 mm, the overall calibration was deemed successful. More observed data points within the study area could further refine the calibration. The model was rerun with the adjusted parameters to enhance its response to flooding events in the study zone.
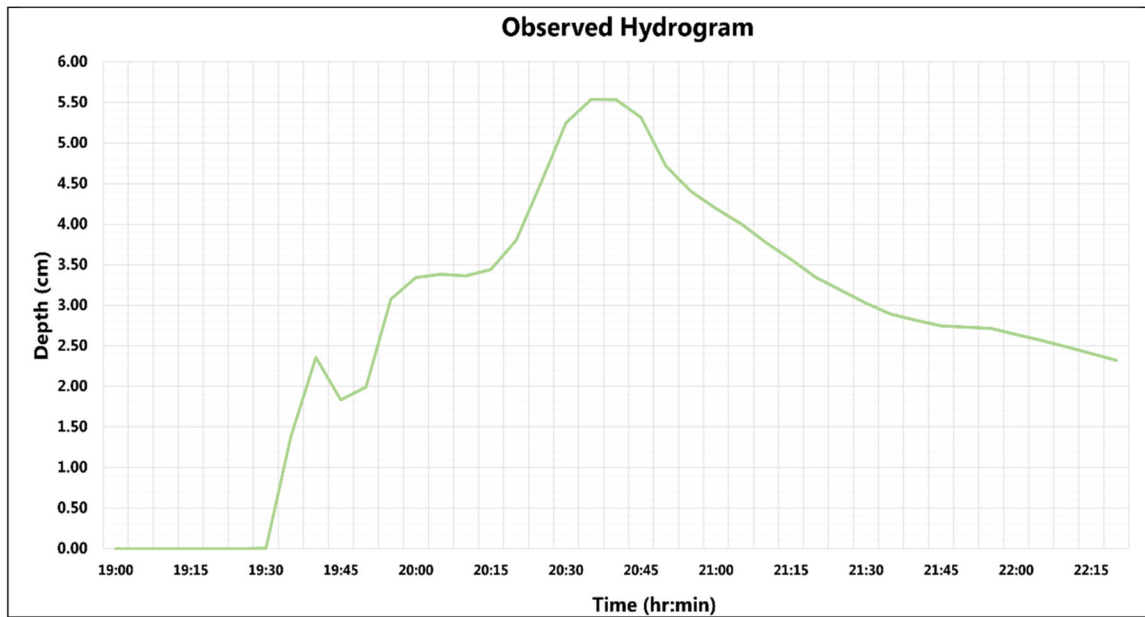
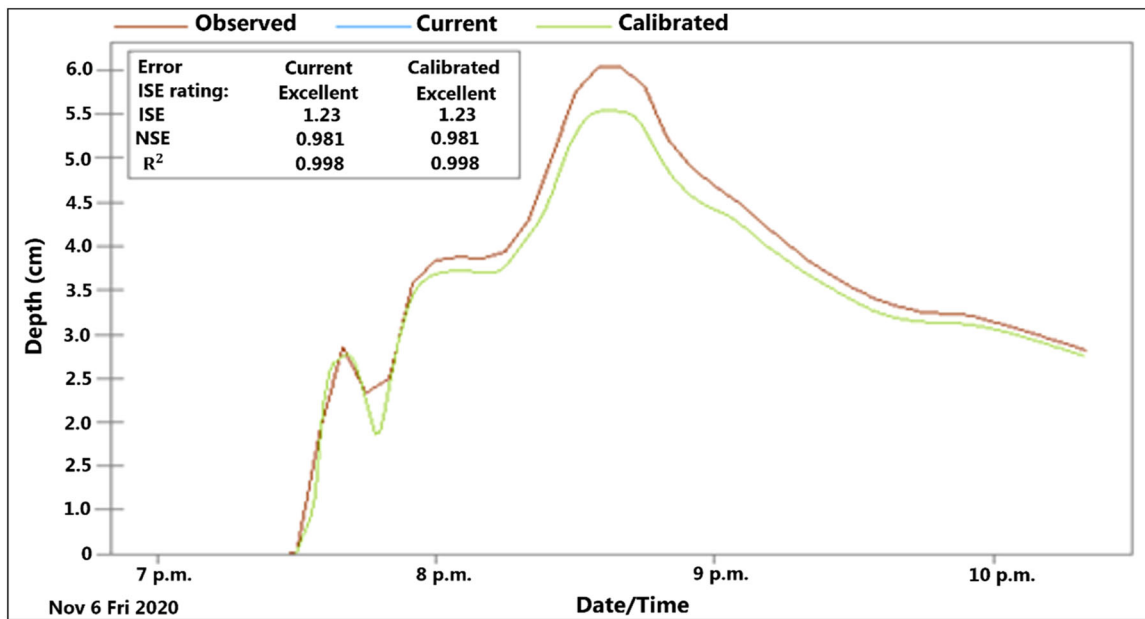**FIGURE 11**   Observed hydrogram of the study zone. *Source*: Authors.

FIGURE 12   Calibration of the model using Sensitivity-based Radio Tuning Calibration tool in PCSWMM. *Source*: Authors.

4.5 | Phase 5: Generation of pedestrian hazard maps in GIS

The hydrological and hydraulic model initially facilitated a spatiotemporal depiction of flash flooding within the study zone, capturing the flow's velocity and depth for varied rainfall scenarios. Figure 13a,b illustrates the velocity and depth maps corresponding to a rain event anticipated once every 10 years, lasting 3 h. It is observed that a consistent pattern emerges across all simulated historical events (5, 10, 50, and 100 years), indicating slower velocities and deeper waters in the basin's central and eastern sections.

The land's incline aids in the flow's progression over time, eventually pooling in lower regions to cause more profound flooding. Central basin flow is channeled toward the Bogotá canal via Libertadores and Guaimaral avenues, thus concentrating a significant volume of rainwater on the roadway and impacting pedestrian safety due to increased velocities.

In Figure 13a, the northeastern sector of the study area (Barrio Zulima, Tasajero neighborhood) exhibits elevated velocity levels, ranging from 0.5 to 1.8 m/s, with certain areas even surpassing 1.8 m/s, indicating a probable heightened risk of pedestrian slippage. These elevated
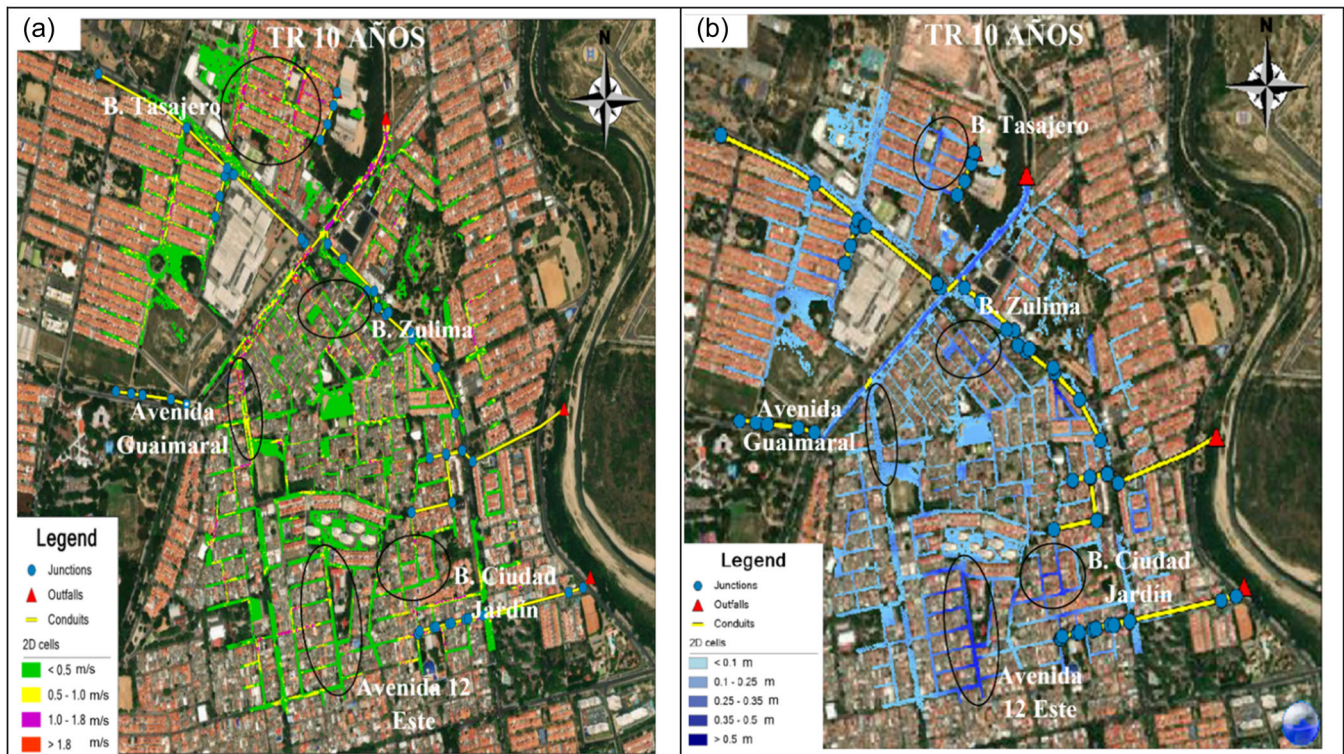
FIGURE 13 Hazard maps for Tr = 10 (a) velocity and (b) water depth.

velocities result from the steep gradients of main roads entering the neighborhood, leading to accelerated flow rates. Near the intersection with the Bogotá Canal and Calle 9b Este on Guaimaral Avenue, velocities exceed 0.5 m/s but remain below 1.8 m/s, posing significant slip risks to pedestrians. In contrast, velocities below 0.5 m/s on other roads suggest safer conditions with minimal slippage risk.

Figure 13b shows that most study area flow depths remain under 0.1 and 0.15 m, implying minimal risk of pedestrian overturn by the flow force and mitigating nearby home damage, as the roadway flow does not surpass curb height. Yet, the flood's breadth across many roads fully spans their width, exceeding Colombia's acceptable flood width. Depths surpassing 0.25 m in Avenida 12 Este and certain Zulima and Ciudad Jardín neighborhood roads, climbing above 0.5 m, significantly increase the likelihood of pedestrian overturn during the crossing. These substantial flow depths are primarily attributed to topographical factors, with minimally inclined roads accumulating runoff, particularly from adjacent streets, exacerbating sector flooding.

Velocities, flow depths, and their product (velocity × depth) were evaluated for streets with significant vehicular and pedestrian traffic within the study area (Avenida 12E, Avenida Guaimaral, and Avenida Libertadores). Figure 14 displays the dynamics of these hydraulic variables across simulated historical events (5, 10, 50, and 100 years), revealing that Avenida 12E is anticipated to exhibit high-risk levels across all return periods. This is attributed to water depths exceeding the threshold defined by the

selected research methodology, indicating a high likelihood of overturning for pedestrians on this avenue. Conversely, for Avenida Guaimaral and Avenida Libertadores, the risk of high danger to pedestrians' hinges on the flood velocities for different return periods. As demonstrated in Figure 14a–d, velocities surpass the established threshold, signifying that pedestrians navigating these avenues could face a heightened risk of slipping in the event of flooding.

Figure 14a–d demonstrates that outliers (marked with asterisks) and extreme values (indicated by circles) are present across all return periods for each evaluated road. Avenida 12E features outliers in velocity ranging from 0.9 to 1.9 m/s. On the other hand, Avenida Guaimaral and Libertadores do not show outliers in velocity but rather in flow depths; their maximum outlier depths being 0.59 and 1.28 m, respectively. It is worth noting that Avenida Guaimaral has extreme values in the interaction of velocity and water depth (v × y), reaching up to approximately 0.60 m²/s, and displays an unusually low velocity of 0.8 m/s. This is in contrast to Avenida Libertadores, which has an extreme minimum velocity of only 0.063 m/s, highlighting the distinct hydrodynamic behaviors across different urban avenues during flood events.

The dispersion of data points suggests there is spatial and temporal variability in each location. This means that at different times during the flood event, each road may experience different velocities and water depths, leading to a spread of v × y values. This variability is crucial for understanding the risk at different times and locations, which is important for flood risk management and urban planning.
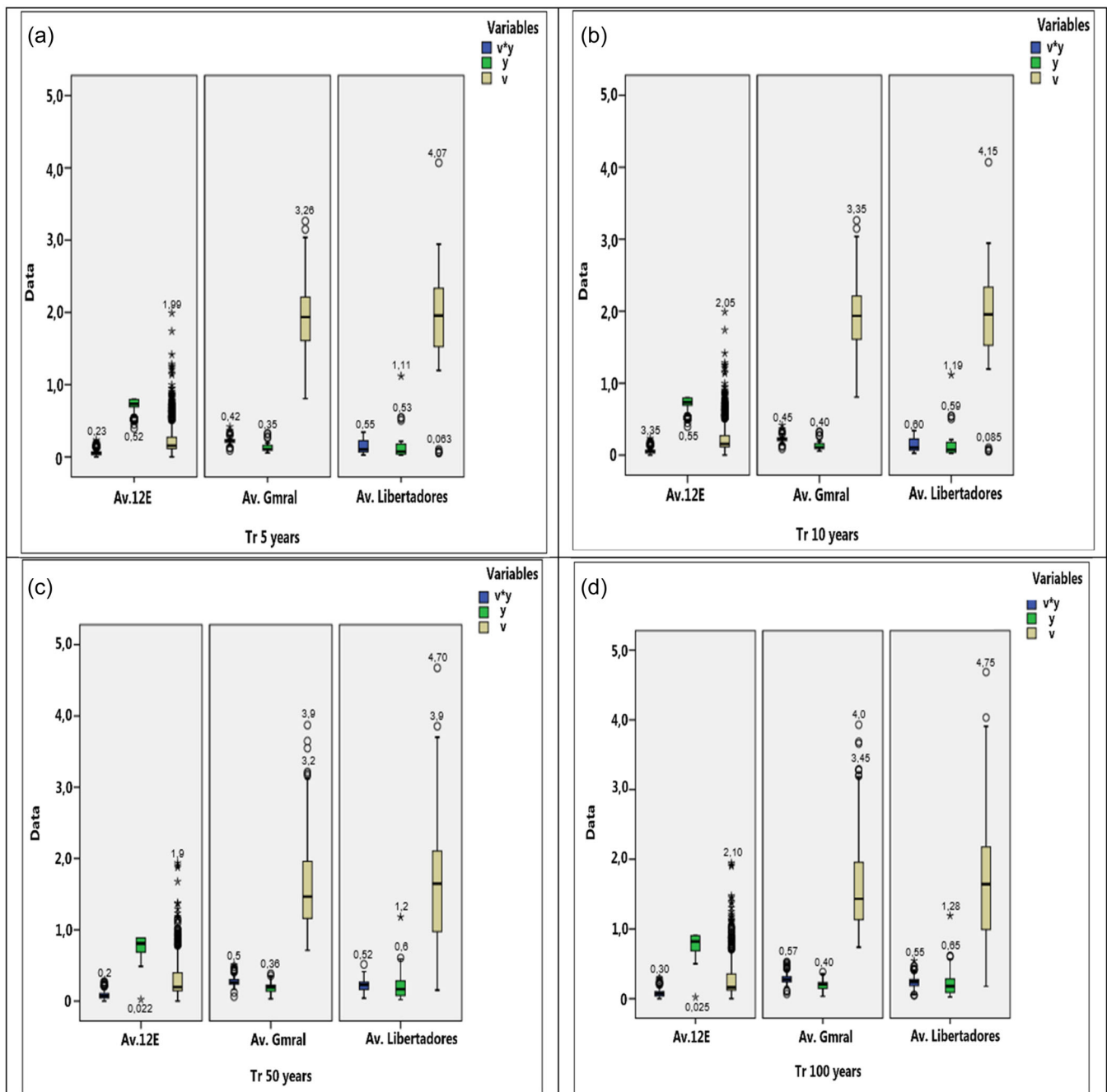
FIGURE 14 Flow velocity and flow depth analysis. (a) 5, (b) 10, (c) 50, and (d) 100 years.

Using the velocity and depth data extracted from the model for each historical event, pedestrian hazard maps were produced in QGIS, spatially depicting areas of potential danger based on the criteria outlined in the methodology.

4.6 | Phase 6: Pedestrian analysis

For the 5-year return period (Tr = 5, Figure 15a), most streets and locations exhibited low hazard levels, with water depths (y) below 0.5 m and the velocity-depth product (v × y) less than 0.16 m²/s. However, moderate hazard levels were identified in specific areas, such as Avenida Guaimaral, due to velocity-depth products nearing 0.19 m²/s. High hazard areas were pinpointed on Avenida 2 Norte and other specific streets, where velocities surpassed 1.8 m/s, reaching up to 2.3 m/s.

The 10-year return period hazard map (Figure 15b) shows low-hazard areas similar to the 5-year map, reflecting the consistent topography of the study area. Nonetheless, areas with medium hazard levels expanded to new sections, and high hazard zones emerged in places with low slopes, where water depths approached 0.65 m, exceeding the methodology's threshold.
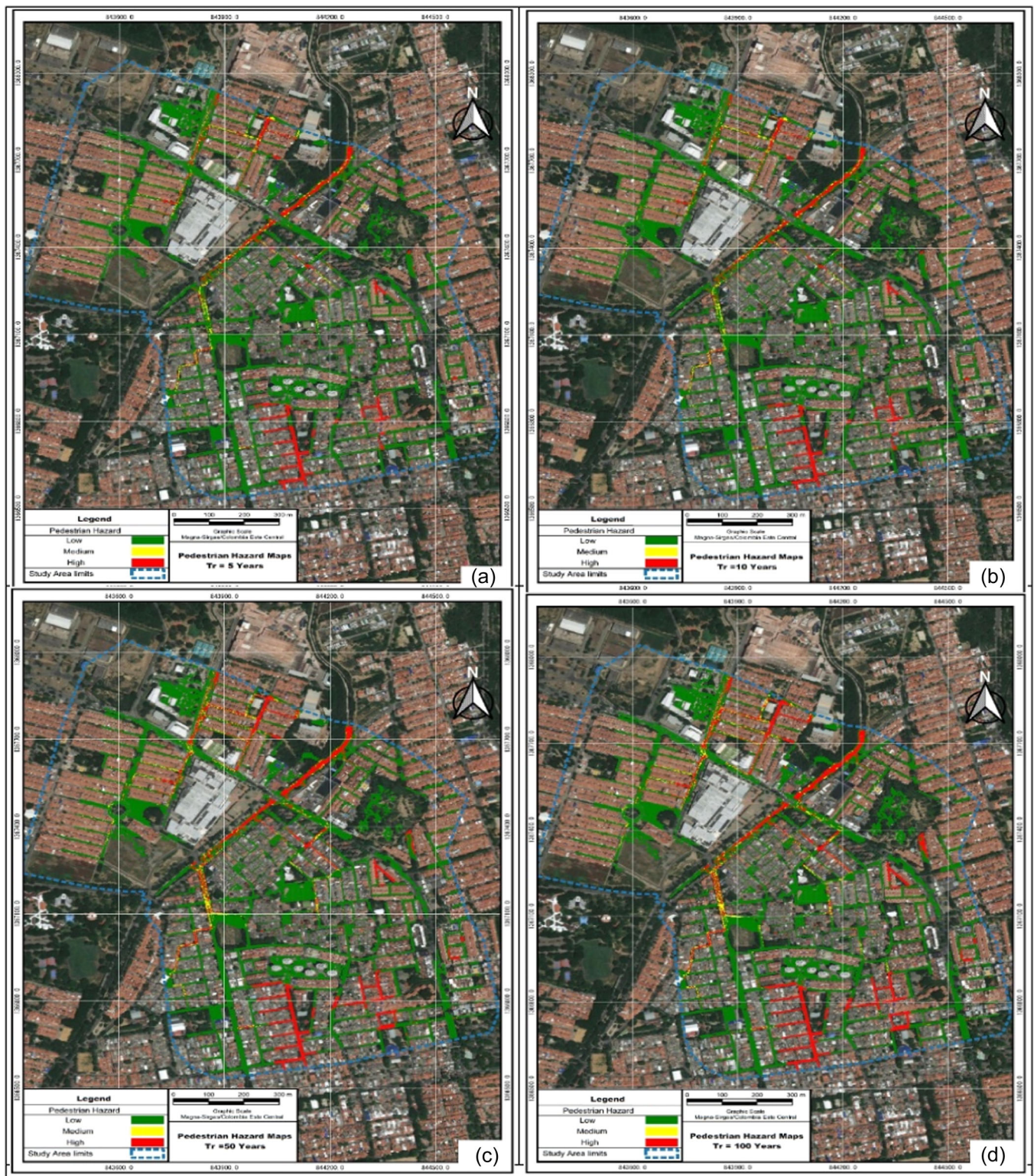
FIGURE 15 Inundation maps (a) 5 years, (b) 10 years, (c) 50 years, and (d) 100 years.

There was a significant increase in areas with medium and high hazard levels for the 50 and 100-year return periods (Figure 15c,d). For instance, certain intersections displayed medium hazard due to velocity-depth products slightly below the high-hazard threshold, while specific avenues showed high pedestrian danger, with maximum velocities reaching up to 3.3 m/s and depths exceeding 0.8 m, well above the established limits.

These maps provide a quantitative assessment of the dangers pedestrians face due to instability during historical rainfall events. In the 5-year event scenario, the majority of the inundated areas, amounting to 88.4%, were considered to

be at low risk, while only 2% were categorized as moderate risk, and 9.6% were considered high risk. As the return period increases to 10 years, there is a notable uptick in higher-risk areas: low-risk zones decrease slightly to 86.7%, moderate-risk areas increase to 2.2%, and high-risk zones rise to 11.1%, which is a 1.5% increase in high-risk classification. More significant changes are observed in the 50 and 100-year scenarios, where the low-risk regions decrease to 81.9% and 80.4%, moderate-risk areas marginally increase to 2.7% and 3%, and the high-risk categories escalate to 15.4% and 16.6%, respectively. This represents a 4.3% and 5.6% increase in high-risk zones compared to the 10-year event, clearly indicating a significant growth in pedestrian danger associated with more severe rainfall events.

5 | CONCLUSION

This research aimed to analyze pedestrian safety in Cúcuta, Colombia, under the scenario of urban flooding through detailed hydraulic and hydrological modeling. The study integrated results from a comprehensive survey and modeling scenarios with 5, 10, 50, and 100-year return periods. It aimed to understand the interplay between urban flooding and pedestrian safety by examining the differences between raw maps on water depth and velocity versus detailed maps that combined information from forces that affect pedestrians. The methodology identified important differences and highlighted the danger zones. Although the percentages of affected areas do not change significantly with different return periods, the location of the risk does. The study also demonstrated that the time variable of pedestrian risk is crucial, making it challenging to integrate space-time for detailed pedestrian analysis. The study shows that the concept of pedestrian risk levels could vary significantly with the simple combination of water depth and velocity seen independently. The study did not cover the information on thresholds for persons and ages of danger fully, but suggested that it be analyzed in the future, together with spatiotemporal analysis. The spatiotemporal analysis should show how the ratios of changes in the area between the instances of time indicate the variation of pedestrian risk and how the peaks and locations can change due to the dynamics of the events. The study did not consider pluvial floods, but we expect the concept of pedestrian risk levels could be more pronounced in such floods.

Results have shown that certain areas in Zulima, Ciudad Jardina, and Avenida 12E in Cúcuta are highly prone to flooding, especially during short but extreme rainfall events lasting about 3 h. While the maximum flood depth can reach up to 0.5 m and the maximum velocity can reach up to 1.8 m/s, these two factors do not occur at the same time and location. Therefore, the risk of pedestrian danger is not present in the entire area covered by these maximums nor at the same time. The combination of both factors can only occur during specific moments of the event, making it essential to consider the pedestrian approach when assessing flood risk in the region.

The maps of pedestrian danger and flood hazard risk in the area provide valuable information for future studies and serve as a basis for considering this element in future flood risk assessments in the region. It is important to note that variations in the balance between water depth and velocity can significantly affect the flood dynamics. Therefore, future studies should consider the spatio-temporal patterns of flood dynamics, timing, and variations in the drainage system's capacity. Additionally, incorporating real-time data could lead to a more dynamic approach to flood risk assessment.

Lastly, an in-depth study of pedestrian responses during flood events would likely improve the model's precision and applicability.

DATA AVAILABILITY STATEMENT
Data available on request due to privacy/ethical restrictions.

ETHICS STATEMENT
None declared.

ORCID
Gerald Augusto Corzo Perez http://orcid.org/0000-0002-2773-7817
Diego Ivan Sanchez Tapiero http://orcid.org/0000-0002-7270-1813
Manuel Antonio Contreras Martínez http://orcid.org/0000-0002-2856-7768
Chris Zevenbergen http://orcid.org/0000-0003-0807-5253

REFERENCES
Abbas, Z., & Jaber, H. S. (2020). Accuracy assessment of supervised classification methods for extraction land use maps using remote sensing and GIS techniques. *IOP Conference Series: Materials Science and Engineering*, 745(1), 012166. https://iopscience.iop.org/article/10.1088/1757-899X/745/1/012166

Altomare, C., Gironella, X., Suzuki, T., Viccione, G., & Saponieri, A. (2020). Overtopping metrics and coastal safety: A case of study from the Catalan coast. *Journal of Marine Science and Engineering*, 8(8), 556. https://doi.org/10.3390/jmse8080556

Aragón-Durand, F. (2014). Inundaciones en zonas urbanas de cuencas en América Latina. Unidad Nacional para la Gestión del Riesgo de Desastres. Recuperado de https://repositorio.gestiondelriesgo.gov.co/handle/20.500.11762/19850

Arosio, M., Arrighi, C., Cesarini, L., & Martina, M. L. V. (2021). Service accessibility risk (SAR) assessment for pluvial and fluvial floods in an urban context. *Hydrology*, 8(3), 142. https://doi.org/10.3390/hydrology8030142

Avila, L., & Avila, H. (2016). *Hazard analysis in Urban streets due to flash floods: Case study of Barranquilla, Colombia*. World Environmental and Water Resources Congress. https://doi.org/10.1061/9780784479889.016

Bernard, M. (1932). Formulas for rainfall intensities of long duration. *Transactions of the American Society of Civil Engineers*, 96, 592–624. https://doi.org/10.1061/TACEAT.0004323

Castro, E., Caetano, A., da Silva, J. J., & Gonçalves, J. R. (2022). Evaluation of hydrological parameters of the Goiana River basin in the State of Pernambuco using the automatic calibration tool of the

hydrodynamic model PCSWMM in multiple fluviometric stations. *Research, Society and Development*, *12*(2), 1–24. https://doi.org/10.33448/rsd-v11i2.25331

Computational Hydraulics Int (CHI). (2023). *Support*. Retrieved from https://www.chiwater.com/Home/About

Diaz Carvajal, Á., & Mercado Fernández, T. T. (2017). Determination of the curve number in the betancí sub-basin (Córdoba, Colombia) by remote sensing and GIS. *Engineering and Development*, *35*(2), 452–470. http://www.scielo.org.co/pdf/inde/v35n2/2145-9371-inde-35-02-00452.pdf

Escalante, J. O., Cáceres, J. J., & Porras, H. (2016). Orthomosaics and digital elevation models generated from images taken with UAV systems. *Tecnura*, *20*(50), 119–140. https://doi.org/10.14483/udistrital.jour.tecnura.2016.4.a09

Hamouz, V., Møller-Pedersen, P., & Merete-Muthanna, T. (2020). Modelling runoff reduction through implementation of green and grey roofs in urban catchments using PCSWMM. *Urban Water Journal*, *17*, 813–826. https://doi.org/10.1080/1573062X.2020.1828500

Isidoro, J. M. G. P., Martins, R., Carvalho, R. F., & de Lima, J. L. M. P. (2021). A high-frequency low-cost technique for measuring small-scale water level fluctuations using computer vision. *Measurement*, *180*(109477), 109477. https://doi.org/10.1016/j.measurement.2021.109477

James, W., Rossman, L. E., & James, W. R. (2010). *User's guide to SWMM5* (Vol. *13*). Ontario. Retrieved from https://www.chiwater.com/Files/UsersGuideToSWMM5Edn13.pdf

Kim, J., Han, Y., & Hahn, H. (2011). Embedded implementation of image-based water-level measurement system. *IET Computer Vision*, *5*(2), 125–133. https://digital-library.theiet.org/content/journals/10.1049/iet-cvi.2009.0144

Kvočka, D., Falconer, R. A., & Bray, M. (2016). Flood hazard assessment for extreme flood events. *Natural Hazards*, *84*(3), 1569–1599. https://doi.org/10.1007/s11069-016-2501-z

Liu, J., Shao, W., Xiang, C., Mei, C., & Li, Z. (2020). Uncertainties of urban flood modeling: Influence of parameters for different underlying surfaces. *Environmental Research*, *182*, 108929. https://doi.org/10.1016/j.envres.2019.108929

Maimone, M., Malter, S., Rockwell, J., & Raj, V. (2019). Transforming global climate model precipitation output for use in urban stormwater applications. *Journal of Water Resources Planning and Management*, *145*(6), 04019021. https://doi.org/10.1061/(ASCE)WR.1943-5452.0001071

Mohd Sidek, L., Chua, L. H. C., Azizi, A. S. M., Basri, H., Jaafar, A. S., & Moon, W. C. (2021). Application of PCSWMM for the 1-D and 1-D–2-D modeling of urban flooding in damansara catchment, malaysia. *Applied Sciences*, *11*, 9300. https://doi.org/10.3390/app11199300

Martínez Gomariz, E. (2016). [Ph.D. Dissertation], *Urban flooding: Hazard criteria and risk assessment for pedestrians and vehicles.*

Department of Civil and Environmental Engineering, Universitat Politècnica de Catalunya. http://hdl.handle.net/2117/106280

Nájera-Ramos, A. (2021). *Methodological proposal for the generation of orthophotos and high resolution digital elevation models through non-photogrammetric drone flights.* Autonomous University of Guerrero. http://ri.uagro.mx/bitstream/handle/uagro/2498/TE_851102_2021.pdf?sequence=1&isAllowed=y

Nkwunonwo, U. C., Whitworth, M., & Baily, B. (2020). A review of the current status of flood modelling for urban flood risk management in the developing countries. *Scientific African*, *7*, e00269. https://doi.org/10.1016/j.sciaf.2020.e00269

OMM. (2014). Atlas of mortality and economic losses from weather. *Climate and Water Extremes*, 1970–2012. https://library.wmo.imt/idurl/4/51415

Pregnolato, M., Ford, A., Glenis, V., Wilkinson, S., & Dawson, R. (2017). Impact of climate change on disruption to urban transport networks from pluvial flooding. *Journal of Infrastructure Systems*, *23*(4), 04017015. https://doi.org/10.1061/(ASCE)IS.1943-555X.0000372

Russo, B. (2009). *Design of surface drainage systems according to hazard criteria related to flooding of urban areas.* [Ph.D. Dissertation] Department of Civil and Environmental Engineering, Universitat Politècnica de Catalunya. https://dialnet.unirioja.es/servlet/tesis?codigo=258828

Shirvani, M., & Kesserwani, G. (2021). Flood–pedestrian simulator for modelling human response dynamics during flood-induced evacuation: Hillsborough stadium case study. *Natural Hazards and Earth System Sciences*, *21*(10), 3175–3198. https://doi.org/10.5194/nhess-21-3175-2021

Tascón-González, L., Ferrer-Julià, M., Ruiz, M., & García-Meléndez, E. (2020). Social vulnerability assessment for flood risk analysis. *Water*, *12*(2), 558. https://doi.org/10.3390/w12020558

United Nations (UN). (2020). *The United Nations world development report 2020: Water and climate change.* https://unesdoc.unesco.org/ark:/48223/pf0000372985

Xu, P., Xie, S., Dong, N., Wong, S. C., & Huang, H. (2017). Rethinking safety in numbers: Are intersections with more crossing pedestrians really safer? *Injury Prevention*, *25*(1), 20–25. https://doi.org/10.1136/injuryprev-2017-042469